Published in final edited form as:
Biochim Biophys Acta. 2010 March ; 1797(3): 360. doi:10.1016/j.bbabio.2009.12.003.

Ascochlorin is a novel, specific inhibitor of the mitochondrial cytochrome bc_1 complex

Edward A. Berry[a], **Li-shar Huang**[a], **Dong-Woo Lee**[b], **Fevzi Daldal**[b], **Kazuo Nagai**[c], and **Nobuko Minagawa**[d]

[a] SUNY Upstate Medical University, 750 East Adams St., Syracuse, NY 13210, USA

[b] Department of Biology, University of Pennsylvania, Philadelphia, PA19104, USA

[c] Research Institute for Biological Functions, Chubu University, Kasugai 487-8501, Japan

[d] Department of Biochemistry, Niigata University of Pharmacy and Applied Life Sciences, Niigata 956-8603, Japan

Abstract

Ascochlorin is an isoprenoid antibiotic that is produced by the phytopathogenic fungus *Ascochyta viciae*. Similar to ascofuranone, which specifically inhibits trypanosome alternative oxidase by acting at the ubiquinol binding domain, ascochlorin is also structurally related to ubiquinol. When added to the mitochondrial preparations isolated from rat liver, or the yeast *Pichia* (*Hansenula*) *anomala*, ascochlorin inhibited the electron transport via CoQ in a fashion comparable to antimycin A and stigmatellin, indicating that this antibiotic acted on the cytochrome bc_1 complex. In contrast to ascochlorin, ascofuranone had much less inhibition on the same activities. On the one hand, like the Q_i site inhibitors antimycin A and funiculosin, ascochlorin induced in *H. anomala* the expression of nuclear-encoded alternative oxidase gene much more strongly than the Q_o site inhibitors tested. On the other hand, it suppressed the reduction of cytochrome *b* and the generation of superoxide anion in the presence of antimycin A_3 in a fashion similar to the Q_o site inhibitor myxothiazol. These results suggested that ascochlorin might act at both the Q_i and the Q_o sites of the fungal cytochrome bc_1 complex. Indeed, the altered electron paramagnetic resonance (EPR) line shape of the Rieske iron-sulfur protein, and the light-induced time resolved cytochrome *b* and *c* reduction kinetics of *Rhodobacter capsulatus* cytochrome bc_1 complex in the presence of ascochlorin demonstrated that this inhibitor can bind to both the Q_o and Q_i sites of the bacterial enzyme. Additional experiments using purified bovine cytochrome bc_1 complex showed that ascochlorin inhibits reduction of cytochrome *b* by ubiquinone through both Q_i and Q_o sites. Moreover, crystal structure of chicken cytochrome bc_1 complex treated with excess ascochlorin revealed clear electron densities that could be attributed to ascochlorin bound at both the Q_i and Q_o sites. Overall findings clearly show that ascochlorin is an unusual cytochrome bc_1 inhibitor that acts at both of the active sites of this enzyme.

Keywords

ascochlorin; cytochrome bc_1 complex; quinol analog inhibitor; Q_o site; Q_i site

Corresponding Author: Nobuko Minagawa, Department of Biochemistry, Niigata University of Pharmacy and Applied Life Sciences, Niigata 956-8603, Japan. Tel.: +81-250-25-5000; fax: +81-250-25-5021. minagawa@nupals.ac.jp.

1. Introduction

Ascofuranone and ascochlorin are antibiotics produced by the phytopathogenic fungus, *Ascochyta viciae*, and both have closely related prenylphenol structures (Fig. 1a and 1b) [1]. Ascofuranone specifically inhibits trypanosome alternative oxidase, and is considered to be a promising candidate as a chemotherapeutic agent against African trypanosomiasis [2, 3]. Kinetic analyses with purified recombinant trypanosome alternative oxidase demonstrated that the site of inhibition of ascofuranone is the ubiquinol binding domain of this enzyme [4].

Ascochlorin was found to inhibit the respiratory chain [5,6], and its chemical structure was determined by X-ray analyses [7,8]. Since then, many structurally related compounds have been isolated from a variety of fungi, including *Fusarium* sp. LL-Z1272 [9], *Colletotrichum* sp. [10], *Cylindrocladium* sp. [11], *Cylindrocladium ilicicola* MFC-870 [12,13], *Acremonium luzulae* [14], and *Verticillium* sp. [15]. Ascochlorin glycoside was also isolated from the insect pathogenic fungus, *Verticillium hemipterigenum* [16]. These compounds have been reported to show antiviral and antitumor activities [6,12,16]. In addition, the independently isolated compounds LL-Z1272γ and ilicicolin D that are responsible for the antifungal activity of the coprophilous fungus *Nigrosabulum globosum* were found to be identical to ascochlorin [13, 17]. Moreover, some members of the ascochlorin family from *Cylindrocarpon lucidum* also inhibit farnesyl-protein transferase enzyme [18]. For example, the 4-*O*-carboxymethylated derivative of ascochlorin (AS-6) has considerable physiological effects on the genetically obese diabetic mouse to reduce insulin resistance [19] and to enhance the Ca^{2+} binding on the plasma membranes of adipocytes [20], and 4-*O*-methyl ascochlorin induces apoptosis in Jurkat cells [21]. Ascochlorin can also suppress activation of the nuclear transcription factor activator protein-1 in several cancer cell lines [22,23], and activate p53 probably as a result of inhibition of mitochondrial respiration [24]. More recently, it has been shown that ascochlorin strongly inhibited ubiquinol oxidases (*E. coli* cytochrome *bo* and *Trypanosoma vivax* alternative oxidase), which is not surprising due to its close structural resemblance to ubiquinol [25].

According to the proton motive Q cycle, the cytochrome bc_1 complex has two quinone binding sites: the Q_o site where ubiquinol is oxidized and the Q_i site where ubiquinone is reduced [26]. A number of inhibitors specific for the Q_o and Q_i sites of the cytochrome bc_1 complex have been studied intensively to understand the Q cycle mechanism of this enzyme [27]. Among them, antimycin A, NQNO*, funiculosin, ilicicolin H, and dichlorophenyl dimethyl urea (diuron) are well-known Q_i site inhibitors [27,28], whereas the Q_o site inhibitors include stigmatellin, various hydroxyquinones and myxothiazol. The latter molecules block the "bifurcated electron transfer reaction" during which one of the two electrons resulting from oxidation of ubiquinol at the Q_o site reduces the Rieske iron-sulfur protein (and subsequently cytochrome c_1) whereas the other electron is recycled back to the quinol pool via the cytochrome *b* hemes. Currently, a significant amount of structural information is available regarding the binding of these inhibitors that exhibit specific modes of actions [29–31]. Generally, the cytochrome bc_1 inhibitors seem to be specific for one of the two active Q centers. With the exception of NQNO [32], none of the inhibitors has so far been reported to bind both at Q_o and Q_i sites simultaneously.

Here we show that ascochlorin is a new kind of specific inhibitor of the cytochrome bc_1 complex as it affects both of the Q_o and Q_i sites. First, the effect of ascochlorin was examined on the respiratory chains of the ascomycetous yeast *Hansenula* (*Pichia*) *anomala* that has a

*Abbreviations: HQNO or NQNO, heptyl or nonyl hydroxyquinoline-N-oxide; nQNO, HQNO or NQNO; DB, 2,3-dimethoxy-5-methyl-6-decyl-1,4-benzoquinone; DBH_2, reduced DB; NHDBT, nonylhydroxydioxobenzothiazole; MCLA, 2-methyl-6-(*p*-methoxyphenyl)-3,7-dihydroimidazo[1,2-α]pyrazin-3-one; MOPS, 3-(*N*-morpholino)propanesulfonic acid; MES, 2-morpholino ethanesulfonate.

cyanide-resistant respiratory pathway catalyzed by an alternative oxidase [33–35]. Considering the previous data that antimycin A highly induced the cyanide-resistant respiratory activity of *H. anomala* (i.e., the expression of the nuclear-encoded alternative oxidase gene), whereas myxothiazol or stigmatellin showed little effect on the expression of this activity [36,37], we thought that ascochlorin might inhibit the fungal cytochrome bc_1 complex through both the Q_i and Q_o sites of the enzyme. Together with additional spectroscopic analyses using the vertebrate and bacterial enzymes, and the X-ray structure of the avian cytochrome bc_1 complex bound with ascochlorin we show that this inhibitor binds to both of the Q_o and Q_i sites of the enzyme.

2. MATERIALS AND METHODS

2.1 Materials

Ascochlorin and its derivatives, and ascofuranone were all isolated and prepared as reported [1,19]. Antimycin A_3, myxothiazol, dithionite, bovine erythrocyte superoxide dismutase, horse heart cytochrome *c*, and 2,3-dimethoxy,5-methyl-, 6-decyl-1,4-benzoquinone (DB) were purchased from Sigma Chemical Co., stigmatellin was from Fluka Biochemica and SF6847 from Wako Pure Chemical Industries, Ltd. Funiculosin and atovaquone were generous gifts from Sandoz and GlaxoSmithKline, respectively. Nonyl-hydroxydioxobenzothiazole (NHDBT) was provided by Dr. Bernard L. Trumpower, Dartmouth Medical School and LL-Z1272ε was kindly provided by Dr. Akira Takatsuki, Hosei University. Azoxystrobin was a gift from Steve Heaney, Zeneca Agrochemicals. Oxidized DB was reduced to DBH_2 by the procedure of Trumpower and Edwards [38].

2.2 Preparation of mitochondria, bacterial chromatophores, and vertebrate cytochrome bc_1 complex

The cyanide-sensitive mitochondrial fraction was prepared from freshly harvested cells of *H. anomala*, as described in our previous report [34]. Succinate-dependent oxygen uptake activity of the yeast preparation was about 0.178 μmol O_2/min/mg protein. The rat liver mitochondrial fraction was prepared from adult male Wistar rats according to the method of Johnson and Lardy [39]. Succinate-dependent oxygen uptake activity of the liver preparation was about 0.155 μmol O_2/min/mg protein. The preparations retained clear respiratory control, and were responsive to ADP addition. Chromatophore membranes from *Rb. capsulatus* cells were prepared as described [40]. The cytochrome bc_1 complexes of chicken and beef were purified as described previously [29,30].

2.3 Induction of cyanide-resistant respiration

Freshly harvested *H. anomala* cells resuspended in 1 ml of 2 mM potassium phosphate buffer (pH 6.5, A_{600} = 25, 52.4 mg wet cells/ml) were shaken aerobically at 30°C for 2 hours with or without the addition of appropriate inhibitors. Fifty-μl samples were withdrawn, and assayed for cyanide-resistant respiratory activity as previously described [33].

2.4 Analytical methods

Oxygen uptake activity was determined polarographically with an oxygen electrode (Model 5331, Yellow Springs Instrument Co., Inc. Ohio) in a 1-ml glass chamber maintained at 30°C. Cyanide-sensitive O_2 uptake was measured in the presence of 50 nM SF6847. Mitochondrial fractions resuspended in 0.3 M sucrose, 10 mM potassium phosphate, 10 mM Tris-HCl, 10mM KCl, 5 mM $MgCl_2$, and 0.2 mM EDTA (pH 7.4) were pre-incubated with the inhibitors, and the reaction was initiated by the addition of respiratory substrates, as indicated in the tables. Cyanide-sensitive and cyanide-resistant O_2 uptake activities were determined according to our previous report [33,34], and the molar concentrations of the inhibitor needed to halve the

uncoupled respiration rate (IC_{50}) were estimated. The relative extent of cytochrome *b* reduction was determined at 30°C using a stirred cuvette in a Hitachi 557 spectrophotometer, operating in the dual-wavelength mode using the 560–575 wavelength pair. The *H. anomala* mitochondrial fraction (5.46 mg) was suspended in 2 ml of 0.3 M sucrose, 10 mM potassium phosphate, 10 mM Tris-HCl, 10mM KCl, 5 mM $MgCl_2$, and 0.2 mM EDTA (pH 7.4). Estimation of $O_2^{-\bullet}$ generation was carried out using 2-methyl-6-(*p*-methoxyphenyl)-3,7-dihydroimidazo[1,2-α]pyrazin-3-one (MCLA) according to our previously described method [34]. The increase in chemiluminescence intensity (the peak height reflecting $O_2^{-\bullet}$ generation rate) sensitive to 0.5 μM superoxide dismutase was determined.

For EPR spectroscopy, 10 to 30 μM (final concentration) of inhibitor dissolved in dimethylsulfoxide was added to chromatophore membrane samples (approximately 30 mg/ml total membrane proteins concentration). Chemical reduction of the samples was achieved by addition of sodium ascorbate to 5 mM final concentration, and samples were stored in liquid nitrogen until the spectra were recorded. EPR spectroscopy was carried out at sample temperatures of 20 K, 9.44 GHz microwave frequency attenuated to 2 mW of power with modulation amplitudes of 12 Gauss, using a Bruker ESP 300E spectrometer (Bruker Biosciences, Inc.), fitted with an Oxford Instrument ESR-9 helium cryostat (Oxford Instrumentation, Inc.), as reported in [41].

Time-resolved, light activated kinetic spectroscopy was performed on a dual wavelength kinetic spectrophotometer with chromatophore membranes resuspended in 50 mM MOPS buffer (pH 7.0) containing 100 mM KCl for the Q_o site-mediated forward reactions as described in [42], or in 50 mM Glycine-NaOH buffer (pH 9.5) containing 100 mM KCl and 10 μM myxothiazol for the Q_i site-mediated reverse reactions as described in [43,44] in the presence of the following redox mediators (with their respective $E_{m,7}$): 100 μM ferricyanide (FeCN, 430 mV), 8 μM 2,3,5,6-tetramethyl-*p*-phenylenediamine (DAD, 260 mV), 6 μM 1,2-naphthoquinone (NQ, 145 mV), 1 μM phenazine methosulfate (PMS, 80 mV), 1 μM phenazine ethosulfate (PES, 50 mV), 6 μM 2-hydroxy-1,4-naphthoquinone (HNQ, −145 mV), 6 μM benzyl viologen (BV, −359 mV), and a membrane potential uncoupler (2.5 μM valinomycin), as described [45].

The amount of chromatophore membranes used in each assay was normalized to the reaction center content, as determined by measuring the flash induced optical absorbance difference between 605 nm and 540 nm at an E_h of 380 mV, and using an extinction coefficient of 29.8 $mM^{-1}cm^{-1}$. Transient cytochrome *c* re-reduction and cytochrome *b* reduction kinetics were monitored at an ambient potential of 100 mV for the forward reaction, and at 125 mV for the reverse reaction, respectively. The cytochrome *c* and cytochrome *b* kinetics were initiated by a short saturating flash (~8 μs) from a xenon lamp and followed at 550–540 nm and at 560–570 nm, respectively. Antimycin, myxothiazol and stigmatellin used as indicated at 20, 10, and 10 μM, respectively. Ascochlorin was added at a final concentration of 1 or 10 μM, as indicated.

Inhibition of the cytochrome *b* reduction through both Q sites (“double-kill” experiment) by ascochlorin was measured using purified bovine cytochrome bc_1 complex. The enzyme was diluted to 3 or 6 μM in 20 mM potassium MOPS buffer (pH 7.2) containing 100 mM NaCl, 0.5 mM EDTA, and 0.1 g/L dodecyl maltoside. Spectra were scanned in the range 520–580 nm before and at ~18 s intervals after addition of the ubiquinol analog DBH_2 (~2 μM) using an Aminco DW2 specrophotometer operating in the double beam mode. The fully oxidized spectrum was subtracted from all. Difference spectra (Fig. 4) were decomposed into difference spectra of the individual cytochromes to determine the reduction level of cytochromes c_1, b_H, and b_L by the generalized inverse matrix method of [46] using the “scanedit” program available at sourceforge.net (http://scanedit.sourceforge.net/). The standard difference spectra

of the pure cytochromes for use in this method were determined from a global fit to whole-spectral titrations of purified bovine bc_1 complex, as described for the potato bc_1 complex [47] and are included in supplemental materials for this paper. Where antimycin and azoxystrobin were included (panels A and B of Fig. 4), the red-shift spectrum of the appropriate inhibitor was also included in the standard spectra used for analysis.

For structural studies, the chicken cytochrome bc_1 complex was crystallized as described in [29], or by using a slight modification to be reported (manuscript in preparation). After crystallization, ascochlorin was added to the mother liquor at a stoichiometry of three molecules of inhibitor per monomer of the cytochrome bc_1 complex. Inhibitor-soaked crystals were cryo-protected by dipping in a solution of 25% glycerol, 12% polyethylene glycol 4000, 10 mM potassium MES (pH 6.7), 3 mM NaN_3, and 0.1 g/l dodecyl maltoside before freezing in liquid nitrogen for cryogenic data collection. Diffraction data were collected at beamline 5.0.2 at the ALS. The best diffraction datasets were solved by rigid-body refinement of the available chicken cytochrome bc_1 complex structure (PDB accession code: 3H1J) against the new data followed by cycles of automated refinement (positional and individual atomic B-factor refinement) and manual rebuilding. Strong non-crystallographic symmetry restraints were imposed during positional refinement, but not during B-factor refinement. The best dataset was refined to R and Rfree of 0.267 and 0.295, respectively, for 125,000 unique reflections at resolution between 30 and 3.21 Å. Statistics from data processing and structure refinement are presented in Table 6, and the structure has been deposited to the PDB with accession code 3H1L.

3. Results

Table 1 illustrates the inhibitory effects of ascochlorin on the O_2 uptake activities of *H. anomala* mitochondria using five kinds of respiratory substrate. Clearly, ascochlorin inhibited strongly all O_2 uptake activities in a manner comparable to the inhibition by antimycin A_3 and stigmatellin. On the other hand, ascofuranone affected much less the same activities, in spite of its close structural relatedness to ascochlorin. Similarly, the three different derivatives of ascochlorin, which have chemical modifications at the 4-OH group of the benzene ring, also exhibited significantly weaker inhibitor activities.

Next, the effects of ascochlorin on the rat liver mitochondria were examined (Table 2). Comparable to the data shown in Table 1, ascochlorin had potent inhibitory effects, which were similar to those seen with antimycin A_3, stigmatellin, and myxothiazol, whereas ascofuranone had much less effect. Similarly, the three 4-OH derivatives of ascochlorin also exhibited much lower inhibitor activities. Note that the antibiotic LL-Z1272ε differs from ascochlorin by lacking a Cl atom at C5 of the benzene ring with 4′, 5′-dihydrogenated isoprenoid side chain (Fig. 1c). Inhibition of the tested activity by this antibiotic was about 1/300 of that seen using ascochlorin.

Table 3 documents the induction of cyanide-resistant respiratory activity in *H. anomala*, where nuclear-encoded alternative oxidase gene expression is drastically stimulated in the presence of antimycin A [36]. Interestingly, like antimycin A_3, ascochlorin also induced cyanide-resistant respiratory activity. Funiculosin, which had less inhibitory effect on the O_2 uptake activities (Table 1), also induced the alternative pathway but to a lesser extent. In contrast, all of the Q_o site inhibitors tested induced cyanide-resistant respiration only slightly. Thus, like the other Q_i site inhibitors, ascochlorin also seemed to trigger mitochondrial signaling toward the nucleus for increased expression of the alternative oxidase gene in *H. anomala*.

Table 4 documents the suppressive effects of ascochlorin on the cytochrome *b* reduction seen in the presence of succinate and antimycin A_3. The antimycin A_3-dependent reduction of

cytochrome *b* was strongly inhibited following addition of ascochlorin. Considering that myxothiazol also have similar inhibitory effects, this finding suggested that ascochlorin might bind at the Q_o site to block the bifurcated electron flow to the cytochrome *b* like many Q_o site inhibitors. Furthermore, Table 5 shows similar suppressive effects of ascochlorin on antimycin A_3-dependent superoxide anion generation by the *H. anomala* mitochondria. As we reported earlier [34,37], in this species, the rate of superoxide generation is significantly increased in the presence of antimycin A and respiratory substrates. This effect was readily suppressed by ascochlorin in a fashion similar to that observed with myxothiazol or stigmatellin. Recently, antimycin A plus substrate-dependent increase of superoxide production was reported to be suppressed by addition of stigmatellin to bovine heart submitochondrial particles [48]. Thus, our data shown in Tables 4 and 5 suggest that the mode of action of ascochlorin on the cytochrome bc_1 complex is similar to the Q_o site inhibitors.

Ascochlorin affects the EPR lineshape of the reduced Fe_2S_2 cluster

Additional evidence that ascochlorin binds at the Q_o site of the cytochrome bc_1 complex was obtained by comparing the EPR spectra of the reduced Rieske iron-sulfur protein in chromatophore membranes of the photosynthetic bacterium *Rb. capsulatus* recorded in the presence and absence of ascochlorin and other Q_o site inhibitors (Fig 2). Stigmatellin sharpens and shifts towards higher magnetic fields the Rieske ISP g_x EPR transition at g =1.768. On the other hand, myxothiazol, which displaces ubiquinone from the Q_o site, yields a broader signal shifted towards lower magnetic fields. Clearly, ascochlorin also changes the g_x transition of the Rieske ISP, suggesting that it indeed binds to the Q_o site of the cytochrome bc_1 complex. Note that under these experimental conditions the inhibitors that interact with the Q_i site exhibit no effect on the EPR g_x transitions.

Dual-site action in bacterial and vertebrate bc_1 complex

In order to gain insight into the mode of action of ascochlorin at both the Q_o and Q_i sites of the cytochrome bc_1 complex, we monitored the light-induced single turnover cytochrome *c* re-reduction and cytochrome *b* reduction kinetics using chromatophore membranes of *Rb. capsulatus* (Fig. 3). In the absence of any inhibitor, light activation of the reaction center leads to the oxidation of cytochromes *c* that are subsequently re-reduced via the Rieske ISP upon oxidation of QH_2 at the Q_o site. The bifurcated electron transfer that occurs at the Q_o site results in the reduction of cytochrome *b* (*i.e.*, heme b_H), which is then oxidized by the reduction of Q (or SQ) at the Q_i site (Fig. 3A, top panel). The presence of stigmatellin blocks the movement of the Rieske ISP, abolishing cytochromes *c* re-reduction after light activation of the reaction centers, exposing the full extent of cytochromes *c* oxidation. Similarly, addition of antimycin A abolishes oxidation of the cytochromes *b* revealing the full extent of cytochrome *b* reduction (Fig. 3A, top panel). Addition of either 1 or 10 μM ascochlorin inhibited partially or fully the re-reduction of cytochromes *c*, respectively, indicating that Q_o site electron transfer was abolished like stigmatellin (Fig. 3A, middle and bottom panels). Consequently, no cytochrome *b* reduction could be seen, clearly indicating that ascochlorin can bind to the Q_o site to inhibit the cytochrome bc_1 complex. In addition, the extent of cytochromes *c* oxidation mediated by ascochlorin was unlike that seen with myxothiazol, but rather very similar to that seen with stigmatellin. This suggested that ascochlorin also immobilized the Rieske ISP upon its binding to the Q_o site of the cytochrome bc_1 complex.

Next, in order to examine the binding of ascochlorin to the Q_i site, we monitored the Q_i site-mediated reduction of cytochrome *b* (heme b_H) by blocking the Q_o site with myxothiazol (Fig. 3B). For this reverse kinetics, we poised the ambient potential of chromatophore membranes at 125 mV in the alkaline pH (pH 9.5) where the Q_{pool} is fully oxidized. The cytochromes *c* and *b* kinetics of the cytochrome bc_1 complex were then monitored after light activation of the reaction center (Fig. 3B). When the Q_o site was blocked by the addition of myxothiazol,

antimycin A-sensitive reduction of cytochrome *b* through the Q_i site was observed (Fig. 3B, top panel). Remarkably, addition of 1 or 10 μM ascochlorin completely inhibited this cytochrome *b* reduction like antimycin A, indicating that ascochlorin can also bind to the Q_i site under the condition where the Q_o site is blocked (Fig. 3B, middle and bottom panels). Therefore, the light-induced single turnover forward and reverse kinetics clearly showed that ascochlorin can inhibit both the Q_o and Q_i sites reactions catalyzed by the cytochrome bc_1 complex.

The results presented in Figure 4 show that ascochlorin also inhibits at both Q sites in bovine mitochondrial bc_1 complex. Purified complex was treated with either the Q_o site inhibitor azoxystrobin, the Q_i site inhibitor antimycin, or ascochlorin. Spectra were scanned before and after adding a small excess of DBH_2. Because thoroughly mixing in the DBH_2, closing the cuvette chamber, and starting the scan required 15 – 20 seconds, the uninhibited enzyme reactions are essentially complete before the first scan, and the time courses shown represent mainly the slow approach to equilibrium as the quinol reduces cytochrome c_1 by a non-enzymatic mechanism. In the presence of azoxystrobin (Fig. 4A) the Q_o site is blocked. Cytochrome b_H is reduced rapidly before the first scan, while cytochrome c_1 is reduced more slowly by a nonenzymatic mechanism. As this latter reaction raises the potential of the DBH_2/DB couple, cytochrome *b* is partially reoxidized. In the presence of antimycin A (Fig. 4B), both cytochrome c_1 and *b* are rapidly reduced by the bifurcated reaction at Q_o. Due to the oxidant-induced reduction cytochrome b_H is reduced to about 80% level and even cytochrome b_L is reduced nearly 20%. As cytchrome c_1 and the high potential chain are further reduced nonenzymatically, the bifurcated reaction reverses and cytochrome *b* is reoxidized to a level of about 10% reduction within a few minutes. With ascochlorin present, the extent of the rapid reactions is much smaller, with cytochrome c_1 reduced about 20% and cytochrome b_H reduced about 10% by the time of the first spectrum. This is consistent with ascochlorin blocking both Q_o and Q_i sites in most of the complexes, allowing us to do the “double-kill” experiment of Deul and Thorn [49] with a single inhibitor. It might be expected that at subsaturating concentration ascochlorin would bind preferentially to one site or the other, giving characteristics similar to either the azoxystrobin-inhibited or antimycin-inhibited complexes of Fig. 4A and 4B. This was not the case: at lower concentrations the extent of the fast reactions was greater, but as in Fig. 4C the extent of cytochrome c_1 reduction was greater than that of cytochrome b_H (Figure S1). This is characteristic of complexes with both sites active, as the only enzymatic path for cytochrome c_1 reduction is the bifurcated reaction, and the failure of reduced cytochrome *b* to accumulate to the same level implies it is reoxidized by the reaction at Q_i. Increasing the concentration of ascochlorin from 31 to 360 μM further decreased the extent of the fast reactions by about a factor of two compared to Fig. 4C, as also shown in Fig. S1.

Surprisingly, when ascochlorin and antimycin are both present (not shown), there is rapid reduction about half of cytochrome b_H and c_1, even with 240 μM ascochlorin. This peculiar observation may be related to the proposal of Covian et al. [50] that binding antimycin at both Q_i sites allows only one Q_o site to be in an active conformation.

Spectral effects on the *b* hemes

Several inhibitors have been shown to induce changes in the spectra of the reduced *b* cytochromes, usually consisting mainly in a shift of the spectrum toward red or blue wavelengths [51,52]. The change induced by ascochlorin resembles not so much a red-shift as a sharpening up of the alpha peak, with troughs on either side of a peak in the middle. In the absence of other inhibitors, the peak is about 563.5 nm (Fig 5 trace 1–3), and the trough on the long-wavelength side is more prominent. To distinguish effects at the Q_i and Q_o site, ascochlorin was added after saturation of one site or the other with the tight-binding site-

specific inhibitors antimycin and myxothiazol. It has been shown in the case of a number of inhibitors that the spectral effects at Q_o and Q_i sites are additive [52]. Figure 5 shows the effects of antimycin (trace 4) and myxothiazol (6) as well as the further effects induced by adding ascochlorin in the presence of antimycin (5) or myxothiazol (7). Traces 5 and 7 indeed appear slightly different, with the peak to longer wavelengths in the presence of antimycin (when it would be more likely to be interacting with b_L at the Q_o site, and slightly shorter wavelength in the presence of myxothiazol, when it would be interacting with b_H at the Q_i site. However the significance of these differences is uncertain pending further investigation.

Ascochlorin binds in the ionized form

The spectrum of ascochlorin itself is sensitive to pH. Neutral ascochlorin in methanol has an absorbance peak at 295. On addition of NaOH this peak goes away and a significantly more intense one appears at 350 (Fig. S2). This is presumably due to ionization of one or both of the phenolic OH groups, as it is reversible by adding a slight excess of HCl. Since these peaks are in the spectral window between absorbance of protein at 280 nm and the Soret peaks at 315 nm, we can tell whether bound ascochlorin has the spectral characteristics of the neutral or ionized form.

When the neutral form is added to aqueous buffer (20 mM potassium MOPS, pH 7.2, 100 mM NaCl, 0.5 mM EDTA, and 0.1 g/L dodecyl maltoside) at micromolar concentrations, the peak is at 346 (the anionic species, not shown). The peak position is similar (350 nm) when added in substoichiometric amounts to the bovine bc_1 complex at 6 μM (Figure 6), and does not change significantly as excess ascochlorin is added. Although the spectra are noisy in the vicinity of the protein peak at 280 nm, it is clear the inhibitor is not absorbing greatly at 295 nm. This indicates that ascochlorin binds in the ionized form. Alkyl hydroxybenzothiazoles also bind in the ionized form [53].

Crystallographic studies

To confirm the dual sites of action and begin to elucidate the binding mode at each site, crystallographic studies of ascochlorin binding to vertebrate cytochrome bc_1 complex were carried out. The structure of chicken cytochrome bc_1 complex soaked with ascochlorin was solved at 3.21 Å (Table 6). Ascochlorin could be located at two sites in the structure of chicken cytochrome bc_1 complex soaked with the inhibitor, corresponding to the Q_i site and Q_o sites as known from the binding of other inhibitors. Figure 7 shows the position of ascochlorin at these sites in the context of the 3-subunit “catalytic core” of cytochrome *b*, cytochrome c_1, and the Rieske iron-sulfur protein. Figure 8 shows close-ups of the electron density locating the inhibitor, and the derived models at the Q_i (8a, 8b) and Q_o (8c) sites. One notable feature of ascochlorin inhibition is the importance of the Cl atom, as seen for example in the data of Table 2 (compare ascpchlorin and LL-Z1272ε). While the Cl atom could be important for electronic effects on other aromatic ring substituents, the structure seem to suggest (see below) that Cl is actually involved in the interaction with the protein at both sites. If so it is most likely a type of interaction known as the “halide bond” [54]. This interaction involves a polar carbon-halogen bond interacting with electronegative O or N atom. The distance to the latter is somewhat less than the sum of the Van der Waals radii, and the angle C-X-O or C-X-N is approximately linear [54]. Within the limitations of a structure of this resolution, the interactions observed here seem to conform with this description. The data of Tables 1and 2 additionally show that the 4-OH of ascochlorin is important for inhibition.

At the Q_i site, the aromatic ring is sandwiched between the bent-back propionate of heme b_H and the ring of Phe221 of cytochrome *b* (Fig. 8b), apparently H-bonding with His202 and Asp229 (Fig. 8a). The orientation of ascochlorin aromatic ring is not completely unambiguous in this structure. In particular, it is possible that the ring could be flipped 180° compared to the

model shown, or that both orientations are present. Qualitatively though the best fit to the density seems to be obtained with the chloride (Cl) atom making a halide bond [54] with His202 and the OH group *para* to the Cl donating an H-bond to Asp229. In either case, this position corresponds closely to the position of the aromatic ring of ubiquinone seen in crystals of the chicken [55], yeast [56], and bovine [32] cytochrome bc_1 complex and the aromatic salicylamide moiety of antimycin [57]. Interestingly, while the aromatic head-groups of antimycin and ascochlorin lie in the same plane and largely overlap, the alkyl tails (including the dilactone ring of antimycin) leave the head groups at about 90° angles from each other, with antimycin following the groove between helices A and D (and making Van der Waals contact with heme b_H through the crack between them) while the tail of ascochlorin is located more between the helices A and E.

Electron density was also present for ascochlorin binding at the Q_o site. In the presence of ascochlorin the Rieske ISP is found in the cytochrome *b* position, where it forms part of the Q_o site, as with stigmatellin. In structures obtained using this crystal form in the absence of inhibitor or in the presence of "proximal" Q_o inhibitors such as myxothiazol or azoxystrobin, the Rieske ISP is found in the cytochrome c_1 position. Comparing this structure with structures containing stigmatellin, the aromatic ring of ascochlorin is in a position overlapped by the aromatic head of stigmatellin (PDB IDs 2PPJ, 3H1J). An H-bond is clearly present between ascochlorin and His161 of the Rieske ISP, which is one of the 2Fe2S cluster ligands. The other side of ascochlorin ring is in H-bonding distance of a density attributed to Glu272. Although again, the bonding partners cannot be unambiguously identified, the model presented here fits well, with the Cl of the inhibitor bonding Glu272, and its C=O or OH group (or both) binding the His161 N atom of the Rieske ISP. The tail of ascochlorin also overlaps the position occupied by stigmatellin, with the cyclohexyl group at the end of the tail occupying the same space as the two methoxy groups in the tail of stigmatellin. This also corresponds to the position of the second thiazol in the tail of myxothiazol. Clearly there is room for an expansion of the tail at this point. After this point, the tails of stigmatellin and myxothiazol diverge into the bulk lipid phase, but that of ascochlorin does not extend beyond this point.

The involvement of Glu272 is not so clear as in the stigmatellin structures, and probably there is a mixture of conformations. In the first monomer (chain C), there is density that could be the carboxylate of Glu272 H-bonding the inhibitor, but it is not continuous with the backbone of Glu272, and so it has been modeled as a water molecule and Glu272 has been rotated away to the rotamer 3(footnote 2) position. In the second monomer (chain P) it has been modeled as in stigmatellin, with Glu272 in rotamer 4 configuration, making H-bonds with the inhibitor and the N of Glu272.

Discussion

In this work, we have shown that ascochlorin inhibits the cytochrome bc_1 complex by binding at both the Q_i and Q_o sites of the enzyme. Ascochlorin may be a general quinone analog, as it also inhibits the ubiquinone sites in the ubiquinol oxidases (*E. coli bo* and trypanasome alternative oxidase) [25]. In this respect, it resembles the NQNO-type inhibitors that inhibit the complex II, quinol:fumarate reductase [58], formate dehydrogenase, *bo*-type ubiquinol oxidase [59], glycerol phosphate dehydrogenase[60], cytochrome b_6f [61], and both the Q_o and Q_i sites of the cytochrome bc_1 complex [32]. Further, while funiculosin is generally considered to bind at the Q_i site, there have been several reports indicating its interaction with the Q_o site [62–64]. Tsai et al. [62] reported that it also affected the EPR lineshape and midpoint potential of the Rieske ISP, which is structurally distant from the Q_i site and adjacent to the Q_o site.

[2]Side chain conformations are described with reference to the rotamer library distributed with the graphical modeling program O [65], The rotamers are described [66].

Howell and Robinson reported spectral effects of funiculosin, a Q_i site inhibitor on heme b_L near the [63]. Degli Esposti and co-workers [64] suggested that replacement of Ala by Met at a position corresponding to 126 in yeast mitochondrial cytochrome *b* (close to the Q_o site) was partially responsible for resistance to funiculosin in fish. It therefore appears that a group of cytochrome bc_1 complex inhibitors affects both of the active sites of this enzyme. Among them ascochlorin is unusual in that its binding at both of these active sites involves a halide bond with the Cl atom. This bond occurs apparently with a histidine N at the Q_i site, and with a carboxylate or water at the Q_o site, whereas most of the other inhibitors involve an (CH—N), or (CH—O) H-bond, respectively. While the structural details of these bindings are not particularly clear in the current low-resolution structure, this unique information may lead to new approaches for designing inhibitory analogs as drugs and pesticides. Inhibitors that might bind to both of the active sites of the cytochrome bc_1 complex might be invaluable, as occurrence of natural resistance to these kinds of dual action inhibitors would be much lower than those acting only at one of the two sites. Therefore, it will be important to obtain higher resolution data to better define the binding properties of ascochlorin, and in particular, to localize with higher precision the exact location of the Cl atom possibly by using its anomalous signal and greater electron density. At the Q_o site, ascochlorin seems to act like stigmatellin that fixes the Rieske ISP in the cytochrome *b* position, based on the EPR (Fig. 2), the single light-induced forward kinetics (Fig. 3A), and the 3D-structural (Fig. 8c) data. Finally, it is worthy to note that the head group of ascochlorin is shaped more like the ubiquinone head-group as compared with the other inhibitors so far located at the Q_o site, and thus its precise localization might provide a better model for visualizing ubiquinone binding at this active site of the cytochrome bc_1 complex.

Supplementary Material

Refer to Web version on PubMed Central for supplementary material.

Acknowledgments

This research was supported by grants from the Ministry of Education, Culture, Sport, Science and Technology of Japan and by NIH grants DK 044842 to EAB and GM 38237 to FD. We are grateful to Christine Trame and staff at sector 5, the ALS for advice and help in data collection.

References

1. Sasaki H, Hosokawa T, Sawada M. Isolation and structure of ascofuranone and ascofuranol, antibiotics with hypolipidemic activity. J Antibiot 1973;26:676–680. [PubMed: 4792115]
2. Fukai Y, Amino H, Hirawake H, Yabu Y, Ohta N, Minagawa N, Sakajo S, Yoshimoto A, Nagai K, Takamiya S, Kojima S, Kita K. Functional expression of the ascofuranone-sensitive *Trypanosoma brucei brucei* alternative oxidase in the cytoplasmic membranes of *Escherichia coli*. Comp Biochem Physiol 1999;C124:141–148.
3. Minagawa N, Yabu Y, Kita K, Nagai K, Ohta N, Meguro K, Sakajo S, Yoshimoto A. An antibiotic, ascofuranone, specifically inhibits respiration and in vitro growth of long slender bloodstream forms of *Trypanosoma brucei brucei*. Mol Biochem Parasitol 1996;81:127–136. [PubMed: 8898329]
4. Nihei C, Fukai Y, Kawai K, Osanai A, Yabu Y, Suzuki T, Ohta N, Minagawa N, Nagai K, Kita K. Purification of active recombinant trypanosome alternative oxidase. FEBS Lett 2003;538:35–40. [PubMed: 12633849]
5. Tamura G, Suzuki S, Takatsuki A, Ando K, Arima K. Ascochlorin, a new antibiotic, found by the paper disc agar-diffusion method. J Antibiot 1968;21:539–544. [PubMed: 4304615]
6. Takatsuki A, Tamura G, Arima K. Antiviral and antitumor antibiotics. XIV. Effects of ascochlorin and other respiration inhibitors on multiplication of Newcastle disease virus in cultured cells. Appl Microbiol 1969;17:825–829. [PubMed: 4183807]

7. Nawata Y, Ando K, Tamura G, Arima K, Iitaka Y. The molecular structure of ascochlorin. J Antibiot 1969;22:511–512. [PubMed: 5350512]
8. Nawata Y, Iitaka Y. The crystal structure of ascochlorin *p*-bromobenzenesulfonate. Bull Chem Soc Japan 1971;44:2652–2660.
9. Ellestad GA, Evans RH Jr, Kunstman MP. Some new terpenoid metabolites from an unidentified *Fusariu*m species. Tetrahedron 1969;25:1323–1334. [PubMed: 5346204]
10. Kosuge Y, Suzuki A, Hirota S, Tamura S. Structure of colletochlorin from *Colletotrichum nicotianae*. Agric Biol Chem 1973;37:455–456.
11. Kato A, Ando K, Tamura G, Arima K. Cylindrochlorin, a new antibiotic produced by *Cylindrocladium*. J Antibiot 1970;23:168–169. [PubMed: 5465722]
12. Hayakawa S, Minato H, Katagiri K. The ilicicolins, antibiotics from *Cylindrocladium ilicicola*. J Antibiot 1971;24:653–654. [PubMed: 5167226]
13. Minato H, Katayama T, Hayakawa S, Katagiri K. Identification of ilicicolins with ascochlorin and LL-Z1272. J Antibiot 1972;25:315–316. [PubMed: 5042450]
14. Cagnoli-Bellavita N, Ceccherelli P, Fringuelli R, Ribaldi M. Ascochlorin: a terpenoid metabolite from *Acremonium luzulae*. Phytochemistry 1975;14:807.
15. Takamatsu S, Rho MC, Masuma R, Hayashi M, Komiyama K, Tanaka H, Omura S. A novel testosterone 5α-reductase inhibitor, 8′, 9′-dehydroascochlorin produced by *Verticillium* sp. FO-2787. Chem Pharm Bull 1994;42:953–956.
16. Seephonkai P, Isaka M, Kittakoop P, Boonudomlap U, Thebtaranonth Y. A novel ascochlorin glycoside from the insect pathogenic fungus *Verticilliumhemipterigenum* BCC2370. J Antibiot 2004;57:10–16. [PubMed: 15032480]
17. Che Y, Swenson DC, Bloer JB, Koster B, Malloch D. Pseudodestruxins A and B: new cyclic depsipeptides from the coprophilous fungus *Nigrosabulum globosum*. J Nat Prod 2001;64:555–558. [PubMed: 11374942]
18. Singh SB, Ball RG, Bills GF, Cascales C, Gibbs JB, Goetz MA, Hoogsteen K, Jenkins RG, Liesch JM, Lingham RB, Silverman KC, Zink DL. Chemistry and biology of cylondrols: Novel inhibitors of Ras farnesyl-protein transferase from *Cylindrocarpon lucidum*. J Org Chem 1996;61:7727–7737. [PubMed: 11667727]
19. Hosokawa T, Ando K, Tamura G. An ascochlorin derivative, AS-6, reduces insulin resistance in the genetically obese diabetic mouse, *db/db*. Diabetes 1985;34:267–274. [PubMed: 3882494]
20. Hosokawa T, Ando K, Tamura G. Treatment with an ascochlorin derivative, AS-6, increases $^{45}Ca^{2+}$ binding on the plasma membrane of adipocytes in db/db mice. Biochem Biophys Res Commun 1985;127:247–253. [PubMed: 3884007]
21. Tsuruga M, Nakajima H, Ozawa S, Togashi M, Chang YC, Ando K, Magae J. Characterization of 4-*O*-methyl-ascochlorin-induced apoptosis in comparison with typical apoptotic inducers in human leukemia cell lines. Apoptosis 2004;9:429–435. [PubMed: 15192325]
22. Hong S, Park KK, Magae J, Ando K, Lee TS, Kwon TK, Kwak JY, Kim CH, Chang YC. Ascochlorin inhibits matrix metalloproteinase-9 expression by suppressing activator protein-1-mediated gene expression through the ERK1/2 signaling pathway: inhibitory effects of ascochlorin on the invasion of renal carcinoma cells. J Biol Chem 2005;280:25202–25209. [PubMed: 15863510]
23. Nakajima H, Mizuta N, Sakaguchi K, Fujiwara I, Mizuta M, Furukawa C, Chang YC, Magae J. Aberrant expression of Fra-1 in estrogen receptor-negative breast cancers and suppression of the propagation in vivo by ascochlorin, an antibiotic that inhibits cellular activator protein-1 activity. J Antibiot 2007;60:682–689. [PubMed: 18057697]
24. Jeong JH, Nakajima H, Magae J, Furukawa C, Taki K, Otsuka K, Tomita M, Lee IS, Kim CH, Chang HW, Min KS, Park KK, Park KK, Chang YC. Ascochlorin activates p53 in a manner distinct from DNA damaging agents. Int J Cancer 2009;124:2797–2803. [PubMed: 19253369]
25. Mogi T, Ui H, Shiomi K, Omura S, Miyoshi H, Kita K. Antibiotics LL-Z1272 identified as novel inhibitors discriminating bacterial and mitochondrial quinol oxidases. Biochim Biophys Acta 2009;1787:129–133. [PubMed: 19111521]
26. Mitchell P. Possible molecular mechanisms of the protonmotive function of cytochrome systems. J Theor Biol 1976;62:327–267. [PubMed: 186667]

27. von Jagow, G.; Link, TA. Use of specific inhibitors on the mitochondrial bc_1 complex. In: Fleischer, S.; Fleischer, B., editors. Methods in Enzymology. Vol. 126. Academic Press Inc; New York: 1986. p. 253-271.Transport in Bacteria, Mitochondria, and Chloroplasts: Protonmotive Force
28. Gutierrez-Cirlos EB, Merbitz-Zahradnik T, Trumpower BL. Inhibition of the yeast cytochrome bc_1 complex by ilicicolin H, a novel inhibitor that acts at the Q_N site of the bc_1 complex. J Biol Chem 2004;279:8708–8714. [PubMed: 14670947]
29. Zhang Z, Huang L, Shulmeister VM, Chi YI, Kim KK, Hung LW, Crofts AR, Berry EA, Kim SH. Electron transfer by domain movement in cytochrome bc_1. Nature 1998;392:677–684. [PubMed: 9565029]
30. Iwata S, Lee JW, Okada K, Lee JK, Iwata M, Rasmussen B, Link TA, Ramaswamy S, Jap BK. Complete structure of the 11-subunit bovine mitochondrial cytochrome bc_1 complex. Science 1998;281:64–71. [PubMed: 9651245]
31. Kim H, Xia D, Yu CA, Xia JZ, Kachurin AM, Zhang LS, Yu L, Deisenhofer J. Inhibitor binding changes domain mobility in the iron-sulfur protein of the mitochondrial bc_1 complex from bovine heart. Proc Natl Acad Sci USA 1998;95:8026–8033. [PubMed: 9653134]
32. Gao X, Wen X, Esser L, Quin B, Yu L, Yu CA, Xia D. Structural basis for the quinone reduction in the bc_1 complex: a comparative analysis of crystal structures of mitochondrial cytochrome bc_1 with bound substrate and inhibitors at the Qi site. Biochemistry 2003;42:9067–9080. [PubMed: 12885240]
33. Minagawa N, Sakajo S, Komiyama T, Yoshimoto A. Essential role of ferrous iron in cyanide-resistant respiration in *Hansenula anomala*. FEBS Lett 1990;267:114–116. [PubMed: 2114321]
34. Minagawa N, Koga S, Nakano M, Sakajo S, Yoshimoto A. Possible involvement of superoxide anion in the induction of cyanide-resistant respiration in *Hansenula anomala*. FEBS Lett 1992;203:217–219. [PubMed: 1318225]
35. Sakajo S, Minagawa N, Yoshimoto A. Characterization of the alternative oxidase protein in the yeast *Hansenula anomala*. FEBS Lett 1993;318:310–312. [PubMed: 8440388]
36. Sakajo S, Minagawa N, Komiyama T, Yoshimoto A. Molecular cloning of cDNA for antimycin A-inducible mRNA and its role in cyanide-resistant respiration in *Hansenula anomala*. Biochim Biophys Acta 1991;1090:102–108. [PubMed: 1883836]
37. Minagawa, N.; Koga, S.; Nakano, M.; Sakajo, S.; Yoshimoto, A. Generation of superoxide anion detected by chemiluminescence method in the cyanide-sensitive mitochondria and the induction of cyanide-resistant respiration in the yeast, *Hansenula anomala*. In: Yagi, K.; Kondo, M.; Niki, E.; Yoshikawa, T., editors. Oxygen Radicals. Elsevier Science B. V; Amsterdam: 1992. p. 203-206.
38. Trumpower BL, Edwards CA. Purification of a reconstitutively active iron-sulfur protein (oxidation factor) from succinate. cytochrome *c* reductase complex of bovine heart mitochondria. J Biol Chem 1979;254:8697–8706. [PubMed: 224062]
39. Johnson, D.; Lardy, H. Isolation of liver or kidney mitochondria. In: Estabrook, RW.; Pullman, ME., editors. Methods in Enzymology. Vol. 10. Academic Press Inc; New York: 1967. p. 94-96.Oxidation and Phosphorylation
40. Atta-Asafo-Adjei E, Daldal F. Size of the amino acid side chain at position 158 of cytochrome *b* is critical for an active cytochrome bc_1 complex and for photosynthetic growth of *Rhodobacter capsulatus*. Proc Natl Acad Sci USA 1991;88:492–496. [PubMed: 1846443]
41. Cooley JW, Roberts AG, Bowman MK, Kramer DM, Daldal F. The raised midpoint potential of the [2Fe2S] cluster of cytochrome bc_1 is mediated by both the Qo site occupants and the head domain position of the Fe-S protein subunit. Biochem 2004;43:2217–2227. [PubMed: 14979718]
42. Lee DW, Ozturk Y, Osyczka A, Cooley JW, Daldal F. Cytochrome bc_1-c_y fusion complexes reveal the distance constraints for functional electron transfer between photosynthesis components. J Biol Chem 2008;283:13973–13982. [PubMed: 18343816]
43. Saribas AS, Ding H, Dutton PL, Daldal F. Tyrosine 147 of cytochrome *b* is required for efficient electron transfer at the ubihydroquinone oxidase site (Q_o) of the cytochrome bc_1 complex. Biochemistry 1995;34:16004–16012. [PubMed: 8519756]
44. Roberson DE, Dutton PL. The nature and magnitude of the charge-separation reactions of ubiquinol cytochrome c_2 oxidoreductase. Biochim Biophys Acta 1988;935:273–291. [PubMed: 2844257]

45. Dutton PL. Redox potentiometry: determination of midpoint potentials of oxidation-reduction components of biological electron-transfer systems. Methods Enzymol 1978;54:411–435. [PubMed: 732578]
46. Sternberg J, Stillo H, Schwendeman R. Spectrophotometric analysis of multicomponent systems using the least squares method in matrix form. Anal Chem 1960;32:84–90.
47. Berry EA, Huang LS, DeRose VJ. Ubiquinol-cytochrome *c* oxidoreductase of higher plants. Isolation and characterization of the bc_1 complex from potato tuber mitochondria. J Biol Chem 1991;266:9064–9077. [PubMed: 1851164]
48. Dröse S, Brandt U. The mechanism of mitochondrial superoxide production by the cytochrome bc_1 complex. J Biol Chem 2008;283:21649–21654. [PubMed: 18522938]
49. Duel DH, Thorn MB. Effects of 2,3-dimercaptopropanol and antimycin on absorption spectra of heart-muscle preparations. Biochim Biophys Acta 1962;59:426–436. [PubMed: 13885840]
50. Covian R, Gutierrez-Cirlos EB, Trumpower BL. Anti-cooperative oxidation of ubiquinol by the yeast cytochrome bc_1 complex. J Biol Chem 2004;279:15040–15049. [PubMed: 14761953]
51. von Jagow G, Engel WD. Complete inhibition of electron transfer from ubiquinol to cytochrome *b* by the combined action of antimycin and myxothiazol. FEBS Lett 1981;136:19–24. [PubMed: 7319059]
52. Kamensky Y, Konstantinov AA, Kunz WS, Surkov S. Effects of bc_1-site electron transfer inhibitors on the absorption spectra of mitochondrial cytochrome *b*. FEBS Lett 1985;181:95–99. [PubMed: 2982656]
53. Palsdottir H, Lojero CG, Trumpower BL, Hunte C. Structure of the yeast cytochyrome bc_1 complex with a hydroxyquione anion Q_o site inhibitor bound. J Biol Chem 2003;278:31303–31311. [PubMed: 12782631]
54. Auffinger P, Hays FA, Westhof E, Ho PS. Halogen bonds in biological molecules. Proc Natl Acad Sci USA 2004;101:16789–16794. [PubMed: 15557000]
55. Berry EA, Zhang Z, Huang LS, Kim SH. Structures of Quinone binding sites in *bc* complexes: Functional implications. Biochem Soc Trans 1999;27:565–572. [PubMed: 10917643]
56. Hunte C, Koepke J, Lange C, Rossmanith T, Michel H. Structure at 2.3 resolution of the cytochrome bc_1 complex from the yeast *Saccharomyces cerevisiae* co-crystallized with an antibody Fv fragment. Structure 2000;8:669–684. [PubMed: 10873857]
57. Huang LS, Cobessi D, Tung EY, Berry EA. Binding of the respiratory chain inhibitor antimycin to the mitochondrial bc_1 complex: a new crystal structure reveals an altered intramolecular hydrogen-bonding pattern. J Mol Biol 2005;351:573–597. [PubMed: 16024040]
58. Maklashina E, Cecchini G. Comparison of catalytic activity and inhibitors of quinone reactions of succinate dehydrogenase and fumarate reductase from *Escherichia coli*. Arch Biochem Biophys 1999;369:223–232. [PubMed: 10486141]
59. Svensson-Ek M, Brzezinski P. Oxidation of ubiquinol by cytochrome bo_3 from *Escherichia coli*: kinetics of electron and proton transfer. Biochem 1997;36:5425–5431. [PubMed: 9154924]
60. Yeh JI, Chinte U, Du S. Structure of glycerol-3-phosphate dehydrogenase, an essential monotopic membrane enzyme involved in respiration and metabolism. Proc Natl Acad Sci USA 2008;105:3280–3285. [PubMed: 18296637]
61. Lam E. The effects of quinone analogues on cytochrome b_6 reduction and oxidation in a reconstituted system. FEBS Lett 1984;172:255–260. [PubMed: 6745417]
62. Tsai AL, Kauten R, Palmer G. The interaction of yeast Complex III with some respiratory inhibitors. Biochim Biophys Acta 1985;806:418–426. [PubMed: 2982396]
63. Howell N, Robertson DE. Electrochemical and spectral analysis of the long-range interactions between the Q_o and Q_i sites and the heme prosthetic groups in ubiquinol-cytochrome *c* oxidoreductase. Biochem 1993;32:11162–11172. [PubMed: 8218179]
64. Degli Esposti M, Ghelli A, Crimi M, Baracca A, Solaini G, Tron T, Meyer A. Cytochrome *b* of fish mitochondria is strongly resistant to funiculosin, a powerful inhibitor of respiration. Arch Biochem Biophys 1992;295:198–204. [PubMed: 1315503]
65. Jones TA, Zhou JY, Cowan SW, Kjeldgaard M. Improved methods for building protein models in electron density maps and the location of errors on these models. Acta Crystallogr 1991;A47:110–119.

66. Ponder JW, Richards FM. Tertiary templates for proteins: Use of packing criteria in the enumeration of allowed sequences for different structural classes. J Mol Biol 1987;193:775–791. [PubMed: 2441069]

a)

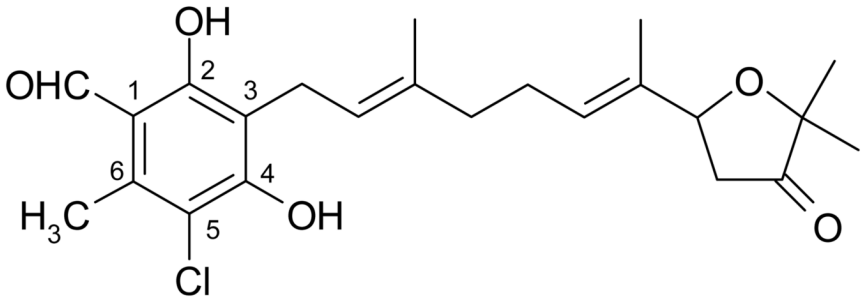

b)

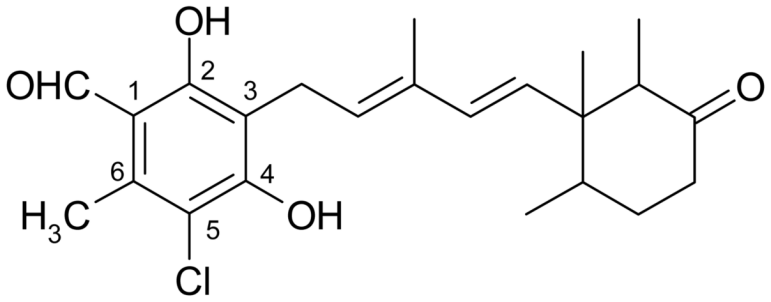

c)

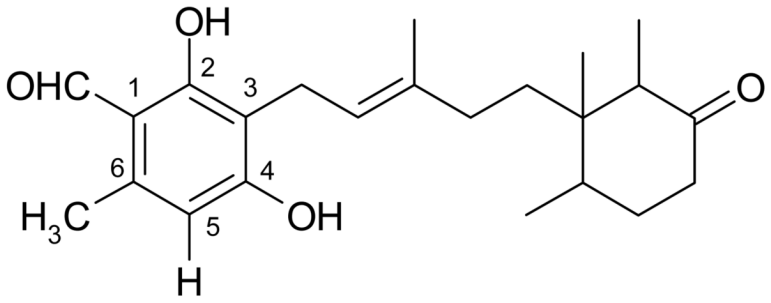

Figure 1. Chemical structures
a) ascofuranone, b) ascochlorin, c) LL-Z1272ε

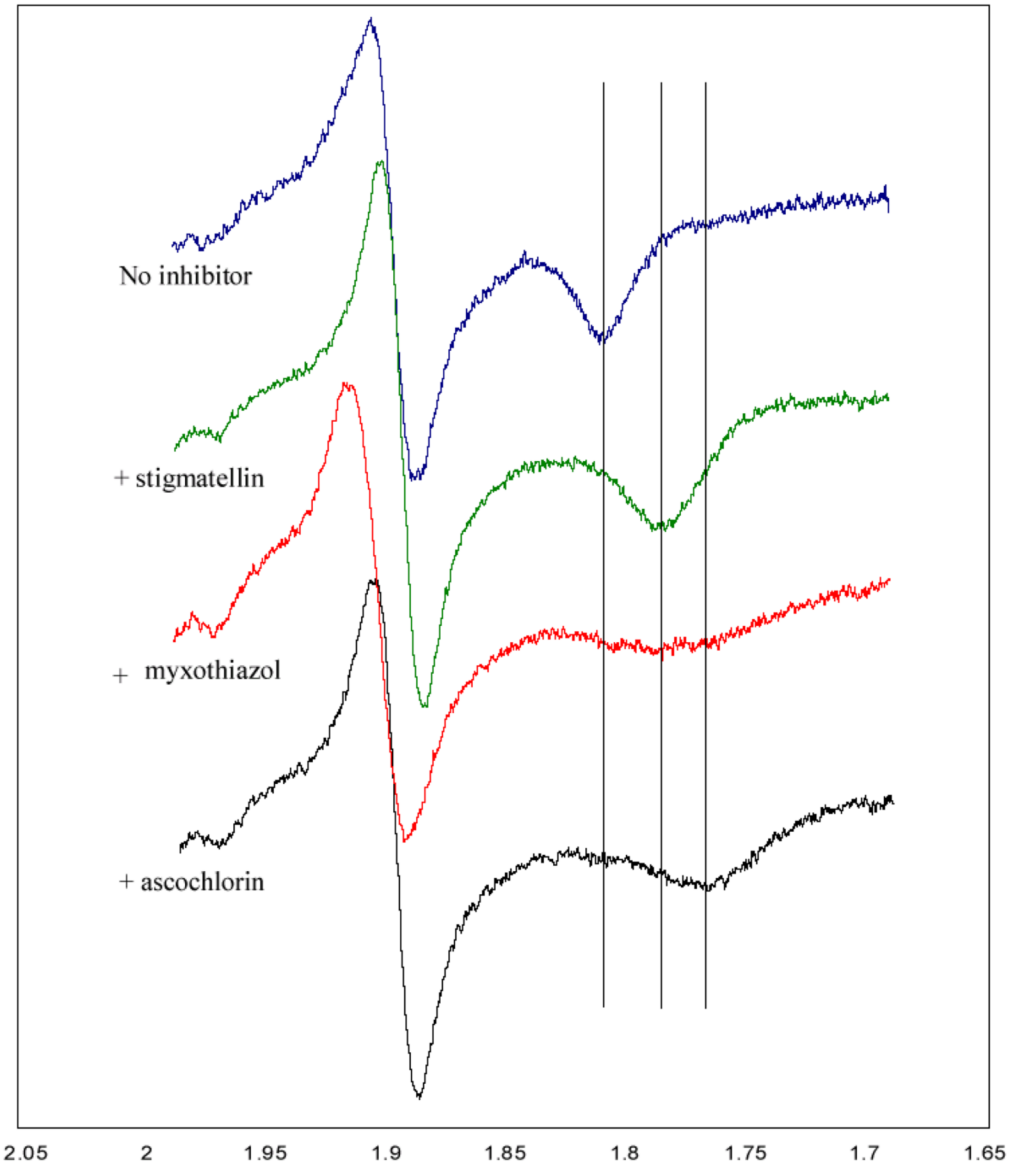

Figure 2.
EPR spectra of the iron-sulfur cluster of *Rb. capsulatusbc* $_1$ complex in the presence of ascochlorin and other ligands.

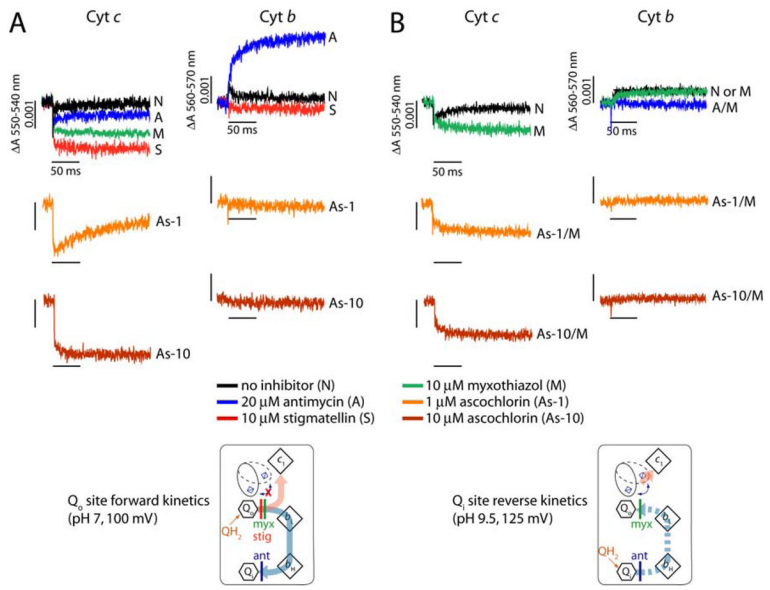

Figure 3. Light-induced, time-resolved single turnover cytochrome *c* re-reduction and cytochrome *b* reduction kinetics of *R. capsulatus*

Chromatophore membranes of *R. capsulatus* containing 0.28 μM reaction center were resuspended in 50 mM MOPS buffer (pH 7.0)/100 mM KCl (A) or 50 mM Glycine-NaOH buffer (pH 9.5)/100 mM KCl/10 μM myxothiazol (B) with appropriate mediators (see "Materials and Methods"). For the forward reaction, the redox potentials were poised at 100 mV where the Q_{pool} is half-reduced and -oxidized at pH 7.0 (A) or at 125 mV where the Q_{pool} is fully oxidized at pH 9.5 (B) for the reverse reaction. Spectral changes were monitored at 550 *minus* 540 nm and 560 *minus* 570 nm for the cytochrome *c* re-reduction and cytochrome *b* reduction following a short (8 μs) flash of light, respectively.

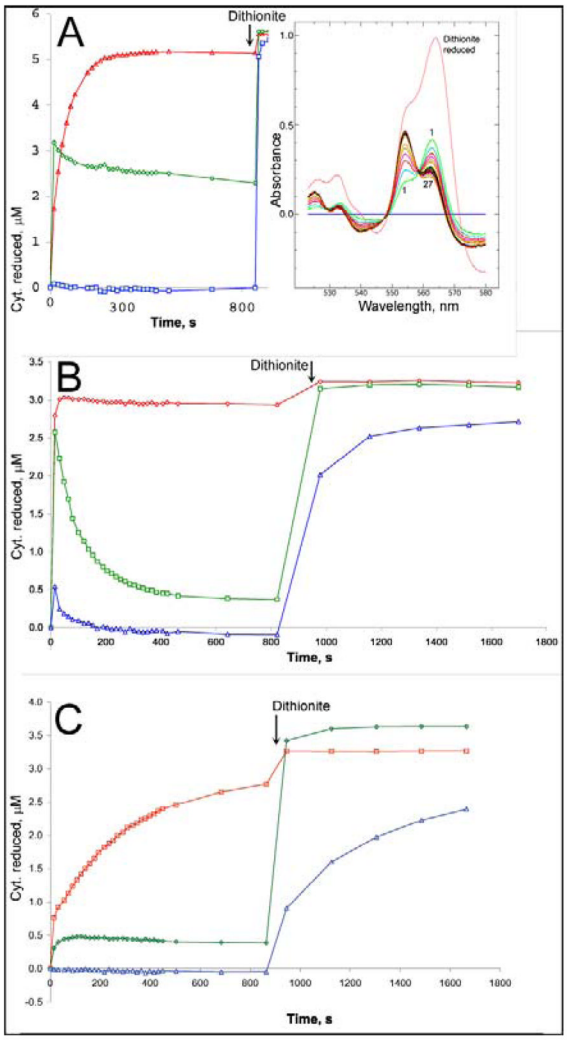

Figure 4. Ascochlorin inhibits reduction of cytochrome *b* in purified bovine cytochrome bc_1 complex through either Q_o or Q_i site

Bovine bc_1 complex was diluted to ~6 μM (A) or 3 μM (B, C) in 20 mM potassium MOPS (pH 7.2), 100 mM NaCl, 0.5 mM EDTA, 5% glycerol, and 0.1 g/L dodecyl maltoside and supplemented with 14 μM azoxystrobin (A), 30 μM antimycin A (B), or 31 μM ascochlorin (C). A preliminary scan (scan 0) showed the complex to be fully oxidized. DBH_2 was added to 25 μM and the sample was scanned repeatedly, at ~18 sec intervals initially, to follow the redox state of the cytochromes. After about 12 minutes, a trace of dithionite was added to the cuvette to determine the maximum extent of reduction. The initial oxidized spectrum was subtracted from all, and the resulting difference spectra (inset in A) were decomposed into sums of the difference spectra of cytochromes c_1 (red), b_H (green), and b_L (blue) as described in "materials and methods" to determine the extent of reduction of each. The results are plotted against time.

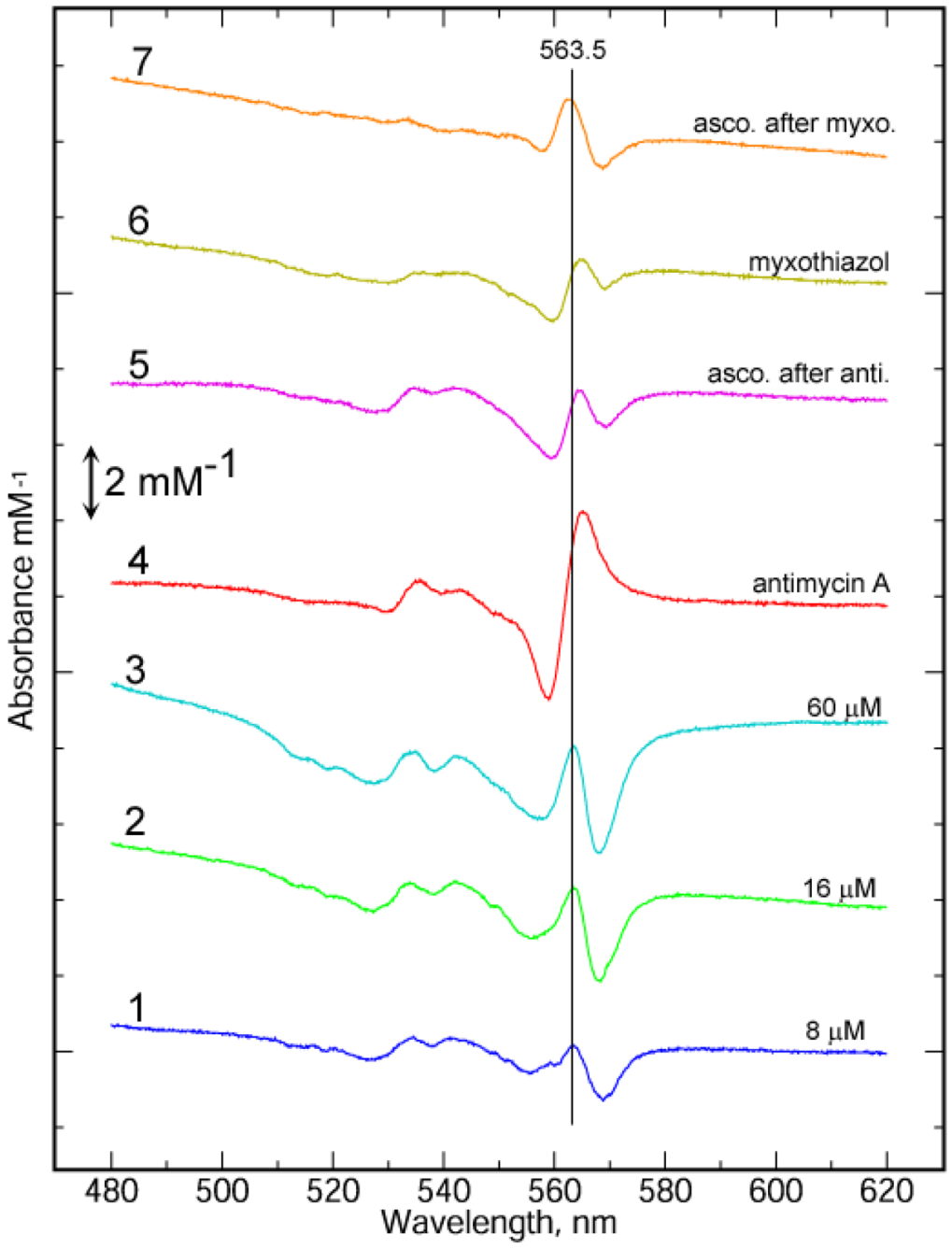

Figure 5. Spectral effects of binding ascochlorin to the reduced bovine bc_1 complex

Bovine bc_1 complex was diluted in 20 mM potassium MOPS (pH 7.2), 100 mM NaCl, 0.5 mM EDTA, 5% glycerol, and 0.1 g/L dodecyl maltoside and reduced with a trace of solid sodium dithionite in an stoppered cuvette. The spectra were scanned until no further change was seen, and then inhibitors were added. For traces 1–3, successive additions of ascochlorin were made to bring the concentration to 8, 16, and 60 μM inhibitor, and spectra were recorded after stabilization. The initial dithionite reduced spectrum was subtracted from each to get the total inhibitor-induced change at each concentration. For traces 4 – 7, 33 μM antimycin (4, 5) or myxothiazol (6, 7) was added, new spectra were recorded, and then 33 μM ascochlorin was added. The spectral changes induced by antimycin and myxothiazol are displayed in traces 4

and 6, respectively. Traces 5 and 7 show the further spectral changes induced by ascochlorin in the presence of antimycin or myxothiazol, respectively. The concentration of bc_1 was 6 μM except traces 4 and 5 (5 μM). The spectra have been divided by the concentration (mM) to allow direct comparison.

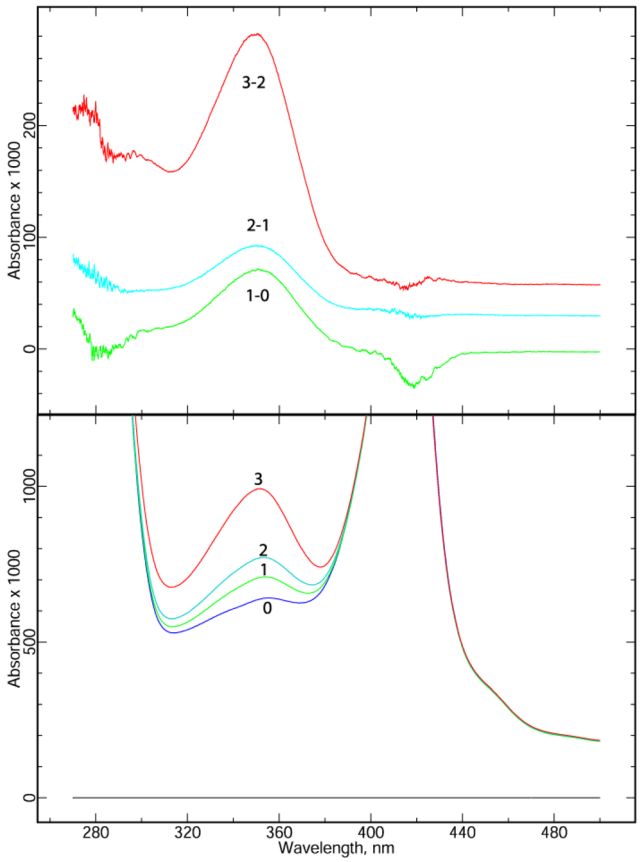

Figure 6. Ascochlorin binds to the bc_1 complex in the ionized form

Bovine bc_1 complex was diluted to 5.8 μM in 20 mM potassium MOPS (pH 7.2), 100 mM NaCl, 0.5 mM EDTA, and 0.1 g/L dodecyl maltoside in a volume of 0.5 ml. A spectrum was recorded (Lower Panel) before (0) and after each of 3 additions: 1 μl of 2 mM (1), 1 μl of 2 mM (2), and 1 μl of 11 mM (3) ascochlorin, bringing the concentration to 4 μM (1), 8 μM (2), and 30 μM (3). Upper Panel: The difference spectra resulting from each of the three additions, (corrected for dilution). The similarity of the change on each addition indicates that bound ascochlorin, like that in neutral aqueous buffer, has spectral characteristics of the ionized form.

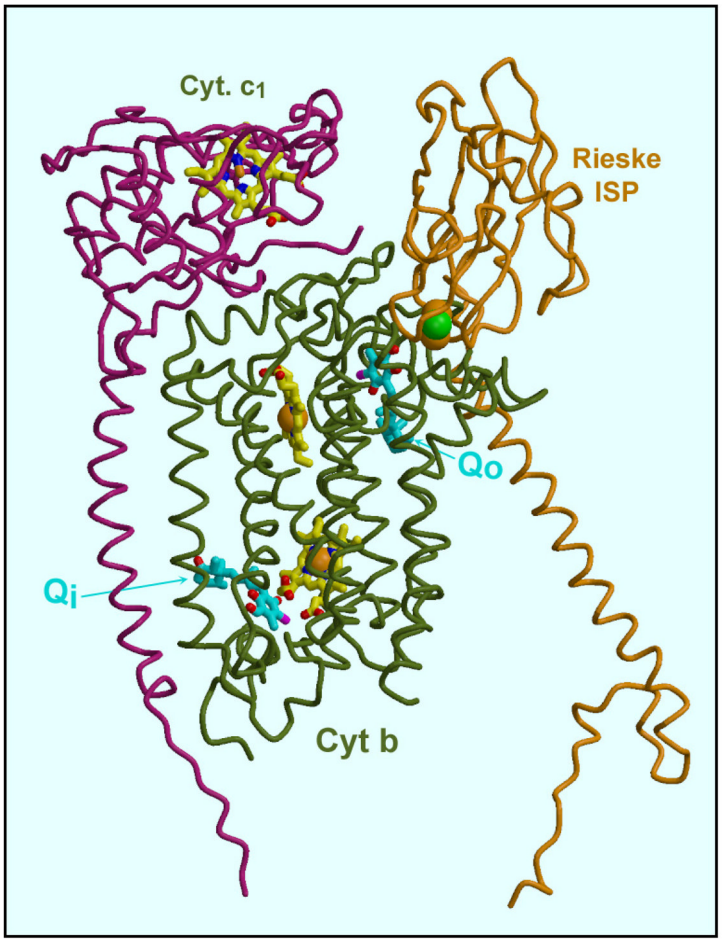

Figure 7. Location of the ascochlorin binding sites within the cytochrome bc_1 complex

The three subunits (cytochrome *b*, cytochrome c_1, and ISP) of a "functional monomer" are shown. The ascochlorin molecules are the yellow ball-and-stick models indicated by "Q_o" and "Q_i" in cytochrome *b*. The blue and yellow ball-and-stick models are (from top to bottom) heme c_1, and heme b_L and b_H of cytochrome *b*. The Rieske iron-sulfur protein is in the cytochrome *b* position, with its cluster (green and yellow spheres) adjacent to ascochlorin at the Q_o site.

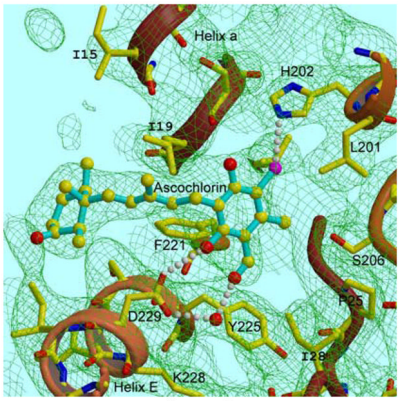

Figure 8a

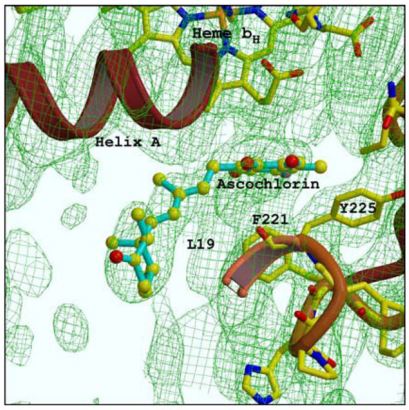

Figure 8b

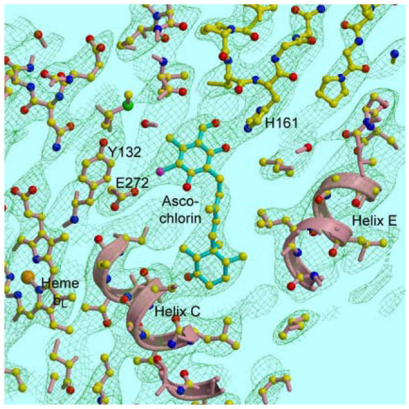

Figure 8c

Figure 8. Electron density at the Q_o and Q_i site of ascochlorin-treated cytochrome bc_1 complex provides evidence for the mode of binding at each site

A, B: Two views of Q_i site. His202, Ser206 and Asp229 are potential ligands. C: Q_o site. His161 of the Rieske iron-sulfur protein, which is in the proximal or "cytochrome *b*" position, ligates substituents on the aromatic ring of the inhibitor. Glu272 of cytochrome *b* shows density for two alternate conformations, the major one (modeled here) forms an H-bond with the other side of the aromatic ring. Electron density is a 2Fo-Fc map contoured at 0.3 e^{-}/A^3.

Table 1

Effects of ascochlorin and related compounds on the O_2 uptake activities of *H. anomala* mitochondria

	IC_{50} (μM)				
Inhibitors	**15 mM Malate + 15 mM Pyruvate**	**15 mM Succinate**	**1 mM NADH**	**1 mM Duroquinol**	**20 mM Glycerol-3-phosphate**
Ascofuranone	230	14.5	68.5	52.0	36.5
Ascochlorin	0.045	0.036	0.035	0.034	0.043
4-*O*-Methyl ascochlorin	5.9	4.8	9.5	4.2	5.8
4-*O*-Carboxymethyl ascochlorin	58.5	43.5	44.0	79.5	22.0
4-*O*-Nicotinoyl ascochlorin	0.37	0.74	0.40	0.60	0.54
Antimycin A_3	0.035	0.020	0.021	0.027	0.026
Funiculosin	0.250	0.145	0.230	0.065	0.195
Stigmatellin	0.042	0.028	0.029	0.030	0.030
Myxothiazol	0.085	0.073	0.069	0.047	0.067

H. anomala mitocondria fraction (0.175 mg protein) was added to the assay mixture. In this preparation, NADH oxidation is catalyzed by rotenone-insensitive external NADH-dehydrogenase.

Table 2

Effects of ascochlorin and related compounds on the succinate-dependent O_2 uptake activity in rat liver mitochondria

Inhibitors	**IC_{50} (μM)**
Ascofuranone	16.0
Ascochlorin (LL-Z1272 γ)	0.013
4-*O*-Methyl ascochlorin	0.120
4-*O*-Carboxymethyl ascochlorin	4.1
4-*O*-Nicotinoyl ascochlorin	0.080
LL-Z1272 ε	3.84
Antimycin A_3	0.0115
Funiculosin	0.280
Stigmatellin	0.014
Myxothiazol	0.0165

The rat liver mitochondria fraction (0.196 mg protein) and 15 mM succinate were added to the assay mixture.

Table 3

Induction of cyanide-resistant respiration in *H. anomala* in the presence of respiratory inhibitors

Additions	**CN^--resistant O_2 uptake activity (nmol O_2/min/mg wet cells)**
None	0.181
10 μM Antimycin A_3	7.77
10 μM Ascochlorin	7.42
10 μM Funiculosin	3.12
10 μM Stigmatellin	0.433
10 μM Myxothiazol	0.375
10 μM Atovaquone	0.202
10 μM NHDBT	0.225

Table 4

Effects of respiratory inhibitors on the reduction of cytochrome *b* in the *H. anomala* mitochondria

Additions	$\Delta A_{560-575} \times 10^2$
15 mM Succinate	0.83
+ 10 μM Antimycin A_3	1.28
+ 10 μM Ascochlorin	0.85
+ Dithionite	1.72
15 mM Succinate	0.92
+ 10 μM Ascochlorin	0.92
+ 10 μM Antimycin A_3	0.94
+ Dithionite	1.76
15 mM Succinate	0.86
+ 10 μM Antimycin A_3	1.27
+ 10 μM Myxothiazol	1.03
+ Dithionite	1.76
15 mM Succinate	0.94
+ 10 μM Myxothiazol	1.16
+ 10 μM Antimycin A_3	1.08
+ Dithionite	1.71

The *H. anomala* mitochondrial fraction (5.46 mg) suspended in 2 ml of 0.3 M sucrose, 10 mM potassium phosphate, 10 mM Tris, 10mM KCl, 5 mM $MgCl_2$, and 0.2 mM EDTA (pH 7.4) was pre-incubated at 30°C, and then 30 μl of 1M sodium succinate was added to the mixture. Absorbance changes were monitored at 560 minus 575 nm as described in “Materials and Methods”. The inhibitors and dithionite were added sequentially as indicated.

Table 5

Superoxide anion generation in the *H. anomala* mitochondria in the presence of respiratory inhibitors

Additions	Chemiluminescence Intensity (10^5 counts/min)
15 mM Succinate	2.0
+ 10 μM Antimycin A_3	9.1
+ 10 μM Ascochlorin	4.6
15 mM Succinate	1.8
+ 10 μM Ascochlorin	2.6
+ 10 μM Antimycin A_3	3.6
15 mM Succinate	1.9
+ 10 μM Antimycin A_3	8.8
+ 10 μM Myxothiazol	5.4
15 mM Succinate	2.1
+ 10 μM Myxothiazol	3.3
+ 10 μM Antimycin A_3	5.6
15 mM Succinate	1.6
+ 10 μM Antimycin A_3	8.9
+ 10 μM Stigmatellin	4.7
15 mM Succinate	1.7
+ 10 μM Stigmatellin	2.7
+ 10 μM Antimycin A_3	4.8

The *H. anomala* mitochondrial fraction (0.18 mg) suspended in 1 ml of 0.3 M sucrose, 10 mM potassium phosphate, 10 mM Tris, 10mM KCl, 0.05 mM $MgCl_2$, and 4 μM MCLA (pH 7.0) was pre-incubated at 30°C in a chemiluminescence reader (Aloka, BLR-102), and then 15 μl of 1M sodium succinate was added to the mixture. The increase in chemiluminescence intensity was determined as described in “Materials and Methods”. The inhibitors were added sequentially as indicated.

Table 6

Key refinement statistics for the Complex III structure with ascochlorin bound at Qo and Qi sites.

PDB Accession code	**3H1L**
Space Group	$P2_12_12_1$
Cell parameters	174.1 × 182.4 × 241.6, 90° 90° 90°
#Atoms refined	32,657
# Reflections	125,125 (16,015)
Resolution range	30 – 3.21
(last shell)	3.37 – 3.21
Completeness	99.1% (91.3%)
Cryst. R Value	0.267 (0.396)
Free R Value	0.295 (0.404)
B Values	
From Wilson Plot	86.7 $Å^2$
Mean atomic B Value	106.4 $Å^2$
RMS Deviations from Ideality:	
Bond Lengths	0.009 Å
Bond Angles	1.4°
Dihedral Angles	21.6°
Improper Angles	0.95°